Soft Matter

Stress Fluctuations in Transient Active Networks

Journal:	*Soft Matter*
Manuscript ID	SM-ART-01-2019-000205.R1
Article Type:	Paper
Date Submitted by the Author:	31-Mar-2019
Complete List of Authors:	Goldstein, Daniel; Brandeis University, Physics Ramaswamy, Sriram; Indian Institute of Science, Physics Chakraborty, Bulbul; Brandeis University

SCHOLARONE™
Manuscripts

Journal Name

Stress Fluctuations in Transient Active Networks[†]

Daniel Goldstein,[*a] Sriram Ramaswamy,[b‡] and Bulbul Chakraborty[a]

Inspired by experiments on dynamic extensile gels of biofilaments and motors, we propose a model of a network of linear springs with a kinetics consisting of growth at a prescribed rate, death after a lifetime drawn from a distribution, and birth at a randomly chosen node. The model captures features such as the build-up of self-stress, that are not easily incorporated into hydrodynamic theories. We study the model numerically and show that our observations can largely be understood through a stochastic effective-medium model. The resulting dynamically extending force-dipole network displays many features of yielded plastic solids, and offers a way to incorporate strongly non-affine effects into theories of active solids. A rather distinctive form for the stress distribution, and a Herschel-Bulkley dependence of stress on activity, are our major predictions.

1 Introduction

Conventional condensed matter can be driven out of equilibrium by forcing at boundaries, e.g. through an imposed difference between velocities[1,2] or temperatures[3]. The result of such external driving can be quite dramatic: solids yield and flow under stress[4,5]; suspensions thin, thicken[6] and band[7,8] under shear; deformation creates and destroys crosslinks in physical gels, leading to viscoelastic properties distinct from polymer melts[9]. Active matter[10–13] refers to condensed systems whose constituents are *self*-driven, that is, they are endowed with a local supply of free energy which they are equipped to convert to directed movement. The question we address in this work is how the strains and stresses generated by active elements lead to transient, elastic networks. Our primary interest is in the stress distributions and intrinsic rheological properties of such a network. This theoretical question has been motivated by experimental observations of spontaneous flow in an isotropic active gel, and the transition from turbulent to coherent flow when these systems are confined[14].

Understanding the development of large-scale flows in active matter is important for many biological systems. The framework of active hydrodynamics[15–18] incorporates the effects of internally generated stress, and has been extraordinarily successful in describing the behavior of self-driven fluids. Active solids have been investigated, in the context of cytoskeleton reorganization[19,20], using hydrodynamic theories. These theories predict the emergence of spontaneous oscillations and travelling waves when motor-driven stresses within the cytoskeleton exceed a threshold. Recent work[20] on the cytoskeleton as an active elastomer includes network rearrangements that reconfigure the connectivity of the actin filaments via crosslinks. This transient network approach is the active analog of theories of viscoelastic response in passive, unentangled but cross-linked polymer networks that reconfigure under external deformations[9]. For a recent review of the rheology of active fluids see[21].

Our work is motivated by a widely studied experimental system consisting of microtubule bundles and motors[14,22–24]. The main features that are of interest to our theoretical work are: (i) The active units are bundles of microtubules (MT) drawn together by depletion forces, and crosslinked by motor clusters that walk along them. The motors induce relative sliding of microtubules with opposite polarity leading, in the experiments[25], to extensile stresses and flow[26]. (ii) When no ATP is supplied to the motors the system behaves as a passive, isotropic gel[14]. (iii) In the presence of ATP, the bundles exhibit a complex dynamics as they extend, bend, buckle, disassemble and reassemble[22]. (iv) There is a bath of polarity-sorted bundles that are not extending, which become incorporated into the network of dynamical bundles. The microtubules are capped[22], therefore, they do not polymerize or depolymerize.

There are features of this experimental system that are difficult to incorporate into existing hydrodynamic theories. For instance, unlike extensile force dipoles, the MT bundles are dynamically extending in length as they exert stresses on their environment. These bundles can also induce states of self-stress in the network due to internal activity. These are states in which stress builds up between two material points while the points remain in force balance, and thus do not move in space[27]. Such states are also not easily incorporated into theories of active fluids. In addition, as

[a] *Martin Fisher School of Physics, Brandeis University, Waltham, USA. E-mail: goldsd@brandeis.edu*
[b] *Centre for Condensed Matter Theory, Department of Physics, Indian Institute of Science, Bangalore 560 012, India.*

discussed above, network rearrangements are not naturally represented in theories of active solids. Motivated by these features, we investigate a microscopic model of transient networks driven by internal extensile activity. This is not meant to be a complete theory since we neglect hydrodynamic interactions and treat the MT bundles as "ghost" filaments without excluded volume interactions. Our objective is to construct a piece of the theory that describes the stress fluctuations originating from active network reorganizations. As we show in this paper, the flows that develop in these transient networks are characterized by stress distributions that are strongly non-Gaussian and whose temporal fluctuations are large and intermittent. Any hydrodynamic theory of these flowing states should account for these rather distinctive stress fluctuations.

2 Model

We model the *passive MT* system by a mechanically rigid *elastic* network of linear springs with spring constants k[27]. Measurements of the mechanical properties of a bundle with two filaments[25] using optical traps show that antipolar arrangements can lead to both extensile and contractile forces. However, at large motor concentrations the length of the bundle grows linearly with time. To model this growth, the equilibrium lengths of the springs, $s(t)$, are programmed to *increase* linearly with time t. The strength of the activity is measured by a single parameter $\alpha = \frac{ds(t)}{dt}$, which is the same for all springs. The nodes in the spring network represent the points of contact between the MTs, where the force is largest.

The observed disassembly and reassembly of the MT[22] suggest that a minimal model should be based on extensile dipoles that are ephemeral: active units can disappear from the network and new ones can be incorporated. When confined within an optical trap[25], the extending bundle buckles and ultimately fails. Force measurements show that the force decreases with buckling before going to zero as the bundle breaks. In our model, we do not include the softening of the spring preceding breakage but incorporate the nonlinearity through the "death" of a spring after a prescribed lifetime.

Bundles with polar arrangements are observed not to extend due to motor activity. We envision these as existing as a bath of springs at their unextended equilibrium length, which can be incorporated into the existing network. When a spring dies, another is "born" and assigned a lifetime τ picked from a distribution, $P(\tau)$, which captures the complex disassembly process observed in experiments[22]. One end of this new spring gets attached to a randomly picked node of the existing network. The number of active springs is thus conserved. The dangling spring becomes completely integrated into the network through a node merging process akin to the crosslinking in passive networks[9]. Nodes that are within a pre-specified merging radius r_*, which is much smaller than the average separation of nodes, are merged and become a new node that inherits all the connections of its parent nodes. The competition of the node merging and the death-birth of springs allows the network to reach a steady state with a well-defined distribution of node connectivity, as shown in the Supplementary Information (SI). The evolution of the network to a steady state
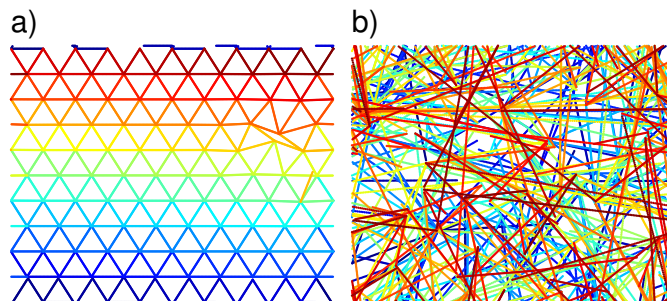
Fig. 1 Snapshots illustrating the transition from the initial network to the flowing steady state. (a) Snapshot just after the first spring has broken. The initial conditions of springs arranged in a triangular lattice with periodic boundary conditions is still seen through the majority of the system. Each spring is assigned a unique color to aid visualization. (b) A snapshot in the steady state, which shows no memory of the initial triangular network. In the SI, we show the connectivity distribution of nodes in the steady state

is illustrated in Fig. 1.

During its lifetime each spring exerts a force on the two nodes to which it is connected, proportional to the difference between its length ℓ (the distance between the two nodes it connects) and its equilibrium length $s(t)$. The nodes evolve with no inertia, i.e. the net force on a node generates a proportionate velocity, not an acceleration.

A simple, illuminating example of how activity can lead to the development of self-stress and network rearrangements is provided by a 1D network with all active springs having the same initial equilibrium lengths s_0 but a distribution of lifetimes. Since the activity α is constant across all springs, they will share the same equilibrium length $s_i(t)$ at time t. Each node will be in force balance as the active stress increases: $\sigma \propto 2k\alpha t$. When the spring with the shortest lifetime fails it is replaced by an unextended spring at unit length at the same position due to the constraints of the one dimensional system. The spring forces on the nodes no longer balance, generating a flow of the nodes towards the "youngest" spring until the next spring breaks. The internal activity can thus lead to "yielding" of the elastic solid in the absence of external stresses. Yielded disordered networks are known to exhibit large-scale spatio-temporal heterogeneities of the stress. As we show below, the yielded active-spring network exhibits a broad distribution of stresses in the steady state.

3 Simulation of 2D network

We evolve the system of active springs using the following rules, which represent the physical processes described in the previous section:

1. Initial state: Create a triangular network of N springs with $s = \ell = 1$, and lifetimes chosen from $P(\tau)$.

2. Calculate the force on node i, $\mathbf{F}_i = \sum_{<ij>} \mathbf{F}_{ij} = k\sum_{<ij>}(s_j - |\ell_j|)\hat{\ell}_j$ where the sum over $< ij >$ counts all the springs j attached to node i.

3. Move all nodes $\mathbf{r}_i(t+\Delta t) = \mathbf{r}_i(t) + \mu\mathbf{F}_i\Delta t$, where μ is the mobility.

4 If two nodes, say i and k, are closer than the threshold merging distance, $|\mathbf{r}_i - \mathbf{r}_k| < r_*$, then merge the nodes. Create a new node at the average position of the two nodes that inherits all the connected springs, then delete the two old nodes.

5 If a spring reaches its lifetime then remove it from the network and introduce a new, unextended spring with $s = \ell = 1$, with one end point chosen randomly from all the nodes in the network and at a random orientation. The other end of the spring is left dangling until a node merger occurs. The lifetime of this new spring is also chosen from $P(\tau)$.

6 Delete any node that has no springs attached to it.

The fifth rule erases any correlation between the lifetime of a spring and its spatial location in the network giving the model a mean-field flavor. The internal stresses in this model, which have elastic and active contributions, are not spatially heterogeneous but display large temporal fluctuations. If, however, the system is confined, then boundary conditions can lead to stress alignment and stress heterogeneities on length scales comparable to the average length that a spring grows to during its lifetime.

We impose periodic boundary conditions in both directions. Unless otherwise stated, results are quoted for a rectangular box with linear dimensions $h = \frac{\sqrt{3}}{2} 50$, and $L = 50$, which accommodates $N = 7500$ springs. Our network-rearranging dynamics conserves the number of springs but not the number of nodes. The distribution of lifetimes is constructed from a Gaussian distribution of the maximum equilibrium length s_{max} with mean $\langle s_{max} \rangle$ and a standard deviation comparable to the mean, which we choose to be $\langle s_{max} \rangle / 4$. Since the activity is the same for all springs, the lifetime is $\tau = (s_{max} - 1)/\alpha$, therefore, $P(\tau)$ is also a Gaussian with mean $\langle \tau \rangle = \frac{\langle s_{max} \rangle - 1}{\alpha}$ and standard deviation $(\alpha \langle \tau \rangle + 1)/4\alpha$. Tuning the activity, α, thus changes the distribution of lifetimes and the network rearrangement dynamics speeds up with increasing activity, as observed in experiments[22]. For any network realization we define the macroscopic stress tensor through the internal virial: $\overleftrightarrow{\sigma} = \frac{1}{A} \sum_{\langle ij \rangle} \mathbf{F}_{ij} \otimes (\mathbf{r}_i - \mathbf{r}_j)$. To examine the viscous response of the system we apply a simple shear through the use of Lees-Edwards boundary conditions[28].

4 Numerical Results

We simulate the model over a range of activities: $\alpha = 0.001$ to $\alpha = 100$, and study the properties of the steady-state that develops after an initial transient. Unless otherwise stated, the numerical results are presented for $\alpha = 1$, $\mu k = 1$, $s_{max} = 10$, and $r_m = 0.01$.

This steady state is usually reached after 2-3 $\langle \tau \rangle$, for N springs with an average lifetime of $\langle \tau \rangle$, which means that on average, every spring has failed at least once before the system reaches steady state. We focus on the stress distribution in steady state. As is well established through theories of active hydrodynamics, these active stresses strongly influence flows. Our approach is distinct from the studies based on hydrodynamics in that we (a) start from the elastic limit, (b) allow the extensile dipoles to grow in length, and (c) incorporate a population of extensile dipoles

within a fluctuating network. These features lead to additional mechanisms of stress generation and instabilities.

We focus on the dynamical properties of the macroscopic stress tensor, since our network reorganization rules wash out any spatial heterogeneities. After the system is initialized, $\overleftrightarrow{\sigma}$ builds up from zero to a steady state value $\overleftrightarrow{\sigma}_{ss}$ about which it fluctuates. This behavior is illustrated in Fig.2a. We can understand the approach to the steady state by considering how the initial triangular network responds to the activity. As the equilibrium lengths of the springs and the stresses borne by them increase, the nodes remain in force balance until the spring with the smallest lifetime breaks (Fig. 1a). The network then rearranges with a sudden release of stress, as a new unstressed spring is introduced. At times long compared to the average lifetime of springs $\langle \tau \rangle$, the network reaches a steady state characterized by a time independent distribution of the ages of the springs (Fig. 1b). The steady-state fluctuations are characterized by an approximately linear rise in the stress between death events, followed by nearly instantaneous stress drops. The average time between these stress drops can be deduced simply by taking the ratio of the average lifetime of a spring, $\langle \tau \rangle$, to the number of springs in the system.

The stress evolution in the active spring model, summarized in Fig. 2, resembles that observed in the yielding of elastic solids[29]. By thinking of the activity as a source of internal strain we can map time to accumulated strain in an elastic solid. In this mapping, the transient of the average stress resembles the elastic branch of a solid and the steady state resembles the yielded state. Instead of being driven to flow by an imposed strain, the elastic network yields due to the internal strains generated by the active springs. This internal driving has no macroscopic anisotropy. Therefore, as shown in Fig. 2(b), we measure the steady-state time average of the trace of the stress tensor, $\langle \Pi \rangle = \mathrm{Tr} \overleftrightarrow{\sigma}_{ss}$, and find that it depends on activity α as $\langle \Pi \rangle = \Pi_p (1 + \alpha^\beta)$ where Π_p is the pressure in the passive limit $\alpha \to 0$. We find $\beta \approx 1/2$: a behavior similar to that observed in yield-stress fluids with α playing the role of strain rate, and Π_p, the yield stress[29]. The relevant timescale comparisons that determine whether this "effective strain rate" is small or large is the ratio of the average lifetime of a spring $\langle \tau \rangle = \langle s_{max} \rangle / \alpha$ to the response time of the spring network $1/\mu k$. For $\langle \tau \rangle << 1/\mu k$, the springs cannot relax between network rearrangement events, which leads to a larger stored stress in the network. Fig. 3 shows the distribution of Π obtained from the time series in steady state. In the rest of the paper, we have scaled $\langle \Pi \rangle$ by Π_p, i.e., we refer to $\langle \Pi \rangle / \Pi_p$ simply as $\langle \Pi \rangle$.

The active springs do not have a yield stress in the traditional sense since their failure is controlled by a preassigned lifetime; however, the network rearrangements lead to stress reorganization and a distribution of effective yield-stresses emerges from the dynamics. We can define this effective yield stress, Π_c, as the trace of self-stress of a spring at the moment it fails: $(\Pi_c)_{ij} = \frac{N}{A} \mathrm{Tr}(\mathbf{F}_{ij} \otimes (\mathbf{r}_i - \mathbf{r}_j))$. The distribution of Π_c in steady state is compared to the distribution of Π in Fig. 2(c). It is seen that the distributions of both Π and Π_c are (i) broad and (ii) asymmetric. The asymmetry is a consequence of the linear-spring forces exerted by the extensile objects in our model. A spring can apply a contractile force if its local environment conspires to stretch is

past its equilibrium length. These contractile forces result in negative stresses. The asymmetry of the stress distributions shows that on average these springs fail while exerting an extensile force. We could have constructed an alternative model where the failure criterion of a spring was determined by its extension, which would be closer to the theories of passive transient networks[9]. In the experiments, however, different mechanisms of failure of the MT bundles are observed. We therefore decided to specify the lifetime distribution. As constructed, the qualitative features of the model are determined by the finite lifetimes of the springs and not by specific failure mechanisms.

In the Supplementary Information, we show that an elasto-plastic model that has been used to simulate plastic flow in soft glassy solids[29,30] qualitatively reproduces the stress distribution and the scaling of stress with activity found in the active spring model if we use as input the observed, emergent, yield stress distribution Π_c (Fig. 2). The strong non-affine effects of the transient network are incorporated in this yield-stress distribution. In the main body of this work we present an alternative stochastic, effective medium model that predicts the stress distribution from the dynamics of the springs without recourse to the yield-stress distribution.

In steady state, springs with widely different lifetimes, τ, sample the same network environment, or conversely a spring with a given lifetime samples widely different network environments. This lack of correlation between spatial location and lifetime suggests that the stress (yield-stress) distribution can be obtained by convolving the stress distribution, *conditioned on the age (lifetime) of a spring*, with the distribution of $t_b = t - t_0$, the time elapsed since the birth of a spring. Since every spring in the system has the same equilibrium-length growth rate α, the conditional stress distribution can be obtained algebraically from the conditional distribution of the lengths $P(\ell, t_b)$ of the springs.

We can accurately fit the numerically measured $P(\ell, t_b)$ (Fig. 3 (a)) by a Gaussian with mean $\mu = at_b + 1$ and variance $D = b_1 t_b + b_2 t_b^2$ (Fig. 3 (c)). Of note is that this mean grows slower than one would expect from a single active spring. Through a change of variables $\Pi(\ell, t_b) = (\alpha t_b + 1 - \ell)\ell$ we then obtain the conditional stress distribution, $P(\Pi, t_b)$. The calculation of the distributions $P(\Pi)$ and $P(\Pi_c)$ by convolving $P(\Pi, t_b)$ with the age distribution of the springs, which is an input to our model, is presented in detail in the SI. Fig. 2(c) compares the numerically measured stress distribution with the forms predicted by the above analysis, and demonstrates that our picture of the steady state applies. The distribution $P(\ell, t_b)$ reflects the different network environments that a spring samples during its lifetime, and is a measure of the disorder in the network that results from the network rearrangements triggered by activity. This is the non-trivial "emergent" property that then controls the stress and yield-stress distributions. This simplicity results from the mean-field character of our model, and we will use it in the next section to provide an effective medium theory of the stress fluctuations.

We have also studied the response of the active springs to external deformations by applying a simple shear strain through the use of Lee-Edwards boundary conditions[28]. As shown in Fig. 2 (d), $\langle\Pi\rangle$ decreases rapidly for $\dot{\gamma}\langle\tau\rangle > 1$ but is insensitive to the
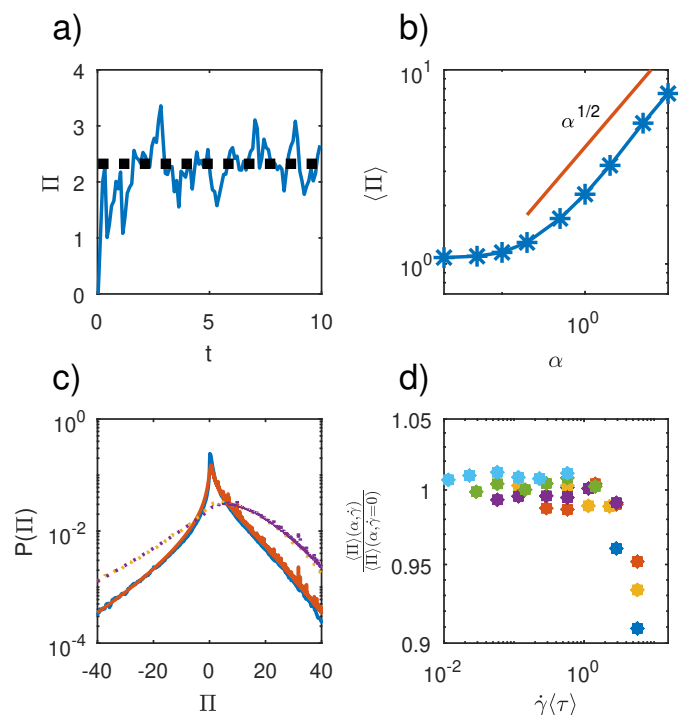
Fig. 2 (color online) (a) A typical time series of the pressure, Π, illustrating a linear stress build up and failure around the global 'yield stress' of the system. (b) Steady state stress $\langle\Pi\rangle$ as a function of the activity. This behavior is well represented by the Herschel-Bulkley law (see text) with activity taking the place of strain rate[29]. (c) Distributions of Π (blue solid) and Π_c (purple dashed) obtained from the simulations compared with those obtained from convolving the stress distributions with the age distribution (see text) (red solid, and orange dashed, respectively). (d) Effect of strain rate $\dot{\gamma}$ on $\langle\Pi\rangle$ is seen to be represented well by the scaling form $\frac{\langle\Pi\rangle(\alpha,\dot{\gamma})}{\langle\Pi\rangle(\alpha,\dot{\gamma}=0)} = g(\dot{\gamma}\langle\tau\rangle)$ with $g(x) \to 1$, $x << 1$ and $g(x)$ decaying rapidly for $x > 1$. In this plot, the colors correspond to different values of α: (blue =0.1, red =0.2 red, yellow = .6 yellow, purple = 1, green =2, and teal = 5)

strain rate for $\dot{\gamma}\langle\tau\rangle << 1$. Recollecting that Π measures the self-stress of the springs, the scaling form demonstrated in Fig. 2 (d) indicates that at shear-rates large compared to their lifetimes, the springs can relax to their equilibrium lengths and, therefore, do not build up stresses. In this limit, the distribution $P(l, t_b)$ resembles that of isolated springs with $\langle l\rangle(t_b) \sim s(t_b)$. The stochastic equations obtained from the effective medium theory presented in the next section support this conclusion.

5 Effective Medium Theory

Each spring in our active network is born with a lifetime picked from a quenched distribution. In addition, when a spring is born, it is attached to a node that is randomly picked from the network. Thus, there is no correlation between the lifetime and the position of a spring. In steady state, therefore, a spring with a given lifetime can be assumed to have sampled all possible network environments. It is therefore natural to formulate an effective medium theory for the distribution $P(\ell, t_b)$. We begin by writing down the dynamics of the end points of a single spring that is not interacting with the network. As there are no externally imposed deformations, we can assume an isotropic system. The dynamics of the length ℓ of a spring, obtained using the force law and

overdamped dynamics is:

$$\frac{d\ell}{dt_b} = 2\mu k(\alpha t_b + s_0 - \ell) \ . \tag{1}$$

Here, s_0 is the equilibrium length that the spring is initialized to at time $t_b = 0$. Solving this equation with $\ell(0) = s_0$ one finds $\ell(t_b) = s_0 + \alpha t_b + \alpha(e^{-2\mu k t_b} - 1)/2\mu k$. There is a slow period for $t_b << 1/2\mu k$ when $\ell(t_b) \simeq s_0 + O(t_b^2)$, and the force exerted on the nodes $\approx \mu k(\alpha t_b + O(t_b^2))$, which is $<< \alpha/2$. For $t_b >> 1/2\mu k$, $\ell(t_b) \simeq s_0 + \alpha t_b - \alpha/2\mu k$, which lags behind the equilibrium length. Therefore, the nodes attached to the spring feel a force $\alpha/2$ away from one another.

In the active-spring network, the length of a spring depends on its connectivity to the network, and the forces exerted by the other springs on the nodes that the spring is attached to. Since a spring with a prescribed t_b is born and samples the network completely randomly, given the rules of the model, we argue that the effect of the other springs can be replaced by a "noisy" elastic medium. The extensile nature of the springs comprising this elastic medium can be incorporated by demanding that the elastic medium pushes out on its surroundings, on average. This medium is thus characterized by an average force that resists compression, and fluctuations of the elastic constant. We model the dynamics of a single spring embedded in such a medium by:

$$\frac{\partial \ell}{\partial t_b} = 2\mu k(\alpha t_b + s_0 - \ell) - \ell \eta \ . \tag{2}$$

Here η is a Gaussian white noise with $\langle \eta \rangle = \omega_\eta$, and a variance $\langle \eta(t)\eta(t') \rangle = 2\omega_c \delta(t-t')$ that characterizes the fluctuations of this elastic medium. The effect of the multiplicative noise is to introduce a *random force* that acts like a spring with a noisy spring

constant and an equilibrium length of zero.

As seen clearly from Eq. 2, the average compressive force exerted by the noisy medium competes with the intrinsic, extensile force due to the activity α. We can develop some intuition about the effect of this multiplicative noise by analyzing the extensional dynamics of a floppy spring ($\mu k = 0$):

$$\frac{\partial \ell}{\partial t_b} = -\ell \eta \ . \tag{3}$$

Making the substitution $\ell(t_b) = e^{z(t_b)}$ it can be seen that z has the same distribution as a Brownian particle with a drift. As shown in the Supplemental Information (SI), the solution for $z(t_b)$ can be used to calculate the average length: $\langle \ell \rangle = \ell(0)\exp(-\omega_\eta t_b + \omega_c t_b)$. On average, the effective medium compresses the floppy spring with a characteristic time scale ω_η. The noise in the effective medium, however, allows the two ends of the floppy spring to extend with a timescale ω_c, mimicking the extensile activity of individual springs. Thus in order to have a medium that resists being compressed on average by the extensile springs, we require $\omega_\eta > \omega_c$. It should be noted that since the "noise" is intended to capture the effects of the effective medium, both ω_η and ω_c should ideally be computed from a self-consistent set of equations that relate them back to $\langle l \rangle$, and $\langle l^2 \rangle$. We have not been able to solve these self-consistency equations, and therefore, have resorted to numerically measuring these noise parameters, which depend on the activity, α, the lifetime distribution, and μk.

Details of the solution to Eq. 2 is provided in the SI. Here, we present the results and compare them to our numerical simulations. The mean length of a spring in this noisy elastic medium is found to be

$$\langle \ell \rangle = \frac{1}{(2\mu k + \omega_\eta - \omega_c)^2}\left[e^{-(2\mu k + \omega_\eta - \omega_c)t_b}\left[(\omega_\eta - \omega_c)(\omega_\eta - \omega_c + 2\mu k)s_0 + 2\mu k\alpha\right] + 2\mu k(2\mu k + \omega_\eta - \omega_c)(s_0 + t_b\alpha)\right] \tag{4}$$

For times $t_b(2\mu k + \omega_\eta - \omega_c) >> 1$ the length is:

$$\langle \ell \rangle = \frac{2\mu k\alpha}{2\mu k + \omega_\eta - \omega_c}t_b \ , \tag{5}$$

where the mean and variance of the noise now affect the speed at which these springs expand. Since $\omega_\eta \geq \omega_c$, the average length is smaller than that of an isolated, extensile object ($\ell \approx \alpha t_b$).

It is convenient to describe the system in terms of two characteristic inverse timescales, or rates: (i) the pure spring elasticity scale, $\omega_{el} = 2\mu k$, and $\omega_{eff} = (\omega_{el} + \omega_\eta - \omega_c)$, the scale characterizing the effective medium, which is a rearranging elastic network. Eq. 5 in this representation gives:

$$\langle \ell \rangle = \frac{\omega_{el}}{\omega_{eff}}\alpha t_b \tag{6}$$

The variance of $P(\ell, t_b)$ can similarly be calculated, but the full form is less useful than the limits. We find that in the small t_b limit

the variance increases linearly with t_b and in the large t_b limit as t_b^2:

$$\lim_{t_b \to 0}\left\langle \ell^2 \right\rangle - \langle \ell \rangle^2 \approx s_0^2 2\omega_c t_b \tag{7}$$

$$\lim_{t_b \to \infty}\left\langle \ell^2 \right\rangle - \langle \ell \rangle^2 \approx \frac{\omega_{el}^2\omega_c}{(\omega_{eff} - \omega_c)\omega_{eff}^2}\alpha^2 t_b^2 \tag{8}$$

As we can see from equations 7 - 8 and Fig 3 (c), the effective medium theory predicts a distribution whose long and short time limit of the mean and variance match the behavior of the measured conditional distributions from the simulation. The distribution of Π, computed from the Langevin equations using values of ω_η and ω_c obtained from fitting $\langle \ell \rangle$ to simulations, compares well with the simulated distribution as shown in Fig. 3 (b). The differences in the negative stress regime indicate that our model
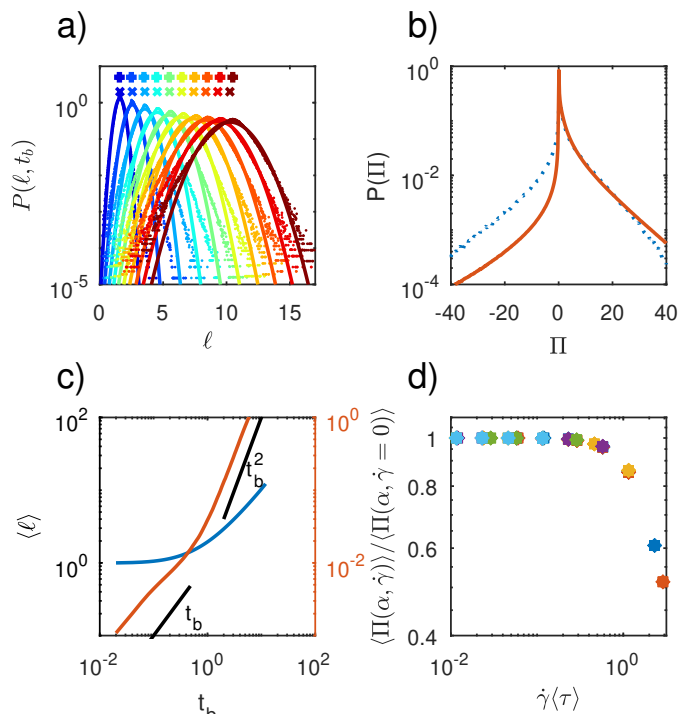
Fig. 3 (a) Spring-length distributions for various t_b with Gaussian fits. Blue corresponds to small t_b and red to large t_b. the x's above the distribution denote the mean and the +'s represent the length of an isolated spring of the same age. Compare to the distribution obtained from the effective medium theory in Fig. ?? (b) Distributions of Π obtained from simulations (blue-dashed) compared to the predictions of the effective medium theory (red-solid). (c) (blue) - The mean of the distribution of spring lengths given that a spring has lived for exactly a time t_b. (red)- The variance of the distribution of spring lengths given that a spring has lived for exactly a time t_b. At small t_b the variance grows linearly and crosses over to quadratic growth at large t_b (d) Effect of strain rate $\dot{\gamma}$ on $\langle \Pi \rangle$ obtained from solving the stochastic differential equations (Eq. 9 and 10). Results follow the scaling form $\frac{\langle \Pi \rangle (\alpha, \dot{\gamma})}{\langle \Pi \rangle (\alpha, \gamma = 0)} = g(\dot{\gamma} \langle \tau \rangle)$ with $g(x) \to 1$, $x << 1$ and $g(x)$ decaying rapidly for $x > 1$. In this plot, the colors correspond to different values of α: (blue =0.1, red =0.2 red, yellow = .6 yellow, purple = 1, green =2, and teal = 5).

of the effective medium as a purely extensile body, which exerts only compressive forces, does not accurately capture the tensile stresses in the springs.

In the SI, we present the numerically measured values of the noise parameters characterizing the effective medium that represents the steady state of the active springs.

To calculate the response to an externally imposed strain, we modify the Langevin equations to incorporate a simple shear in a two-dimensional representation.

$$\frac{dx}{dt} = \cos(\theta)[2\mu k(\alpha t_b + s_0 - \ell) - \ell \eta] + \dot{\gamma} y \qquad (9)$$

$$\frac{dy}{dt} = \sin(\theta)[2\mu k(\alpha t_b + s_0 - \ell) - \ell \eta] \qquad (10)$$

where $\ell = \sqrt{x^2 + y^2}$ and $\theta = \arctan(y/x)$. These equations are not analytically tractable and must be solved numerically. We use the values of ω_η and ω_c obtained from simulations of the active

spring model at $\dot{\gamma} = 0$. Using these parameters, we find that the steady-state average $\langle \Pi \rangle$ follows the same scaling relations observed in the numerical simulations. From the above equations we can deduce that, for $\gamma \langle \tau \rangle >> 1$, the "noise" becomes irrelevant in determining the dynamics, the springs behave as isolated, non-interacting units with their lengths relaxing to their equilibrium length with a timescale $\frac{1}{\dot{\gamma}}$.

To summarize, replacing the network of active springs by an effective medium with "noisy elasticity" yields results for the spring dynamics that agree remarkably well with the full active spring simulations. This stochastic differential equation reproduces the trends in the steady-state averages of the stress in the system and the full stress distribution, qualitatively as shown in Figs. 3(b) & (d). Furthermore the effective medium theory allows us to understand the nature of the stress fluctuations in the system as a result of the interaction of a spring with a noisy elastic medium that exerts compressive forces.

6 Conclusions

Inspired by biological active networks we have created a model to explore the behavior of a network of dynamically extending force dipoles. We have shown that this model shares several characteristics of a yielded plastic solid under periodic boundary conditions. We then show that an effective medium approach using a stochastic differential equation can reproduce key features of the behavior of the system including the effects of external shearing. Since we do not include any hydrodynamic effects, the shear-rate only affects the self-stress of the springs by changing the length distribution of springs that have lived for a prescribed time, $P(l, t_b)$. An effect of the shear-rate that we have not included is restructuring of the bundles themselves. Within our model, this latter effect can be included through a change in the distribution of survival times, $P_s(t_b)$. The mapping of the extensile transient networks to a noisy elastic medium offers an avenue for extending continuum theories of active solids [19,20] to include strong nonaffine effects. These nonaffine effects can be further incorporated into elastoplastic models through yield-stress distributions characteristic of the transient active networks.

Conflicts of interest

There are no conflicts to declare.

Notes and references

1 A Onuki, *J. Phys.: Condens. Matt.*, 1997, **9**, 6119.

2 R M L Evans, R A Simha, A Baule & P D Olmsted, Phys. Rev. E, 2010, **81**, 051109.

3 A Dhar, Adv Phys, 2008, **57**, 457-537.

4 H.A. Barnes, J Non-Newtonian Fluid Mech., 1999, **81**, 133-178.

5 K.H. Nagamanasa, S. Gokhale, A.K. Sood, R. Ganapathy, Phys. Rev. E, 2014, **89**, 062308.

6 E Brown & H M Jaeger, Rep. Prog. Phys., 2014, **77**, 046602.

7 P.D. Olmsted, Rheol Acta, 2008, **47**, 283-300.

8 S M Fielding, Rep. Prog. Phys., 2014, **77**, 102601.

9 F. Tanaka and S. F. Edwards, Macromolecules, 1992, **25**, 1516.

10 S Ramaswamy Annu. Rev. Condens. Matter Phys., 2010 **1** 301.

11 G I Menon, in Rheology of Complex Fluids, eds J Murali Krishnan *et al.*, Springer, New York (2010).

12 É Fodor & M C Marchetti, *The statistical physics of active matter: from self-catalytic colloids to living cells* (Lecture notes for the international summer school "Fundamental Problems in Statistical Physics", Bruneck, 2017); Physica A, 2018, **504**, 106.

13 F. C. MacKintosh, C. F. Schmidt, Current Opinion in Cell Biology, 2010, **22**, 29.

14 K.-T. Wu, J. B. Hishamunda, D. T. N. Chen, S. J. DeCamp, Y.-W. Chang, A. Fernández-Nieves, S. Fraden and Z. Dogic, Science, 2017, **355**, eaal1979.

15 M. C. Marchetti, J. F. Joanny, S. Ramaswamy, T. B. Liverpool, J. Prost, M. Rao and R. A. Simha, Reviews of Modern Physics, 2013, **85**, 1143–1189.

16 David Saintillan & Michael J.Shelley, Comptes Rendus Physique, 2013, **14**, 497.

17 J. Prost, F. Jülicher & J-F. Joanny, Nature Physics, 2015, **11**, 111.

18 F. Jülicher, S. W. Grill and G. Salbreux Reports on Progress in Physics, 2018, **81**, 076601.

19 S. Banerjee and M. C. Marchetti, Soft Matter, 2011, **7**, 463–473.

20 D. S. Banerjee, A. Munjal, T. Lecuit and M. Rao, Nat Commun, 2017, **8**, 1121.

21 D. Saintillan, Annu. Rev. Fluid. Mech., 2018, **50**, 563–592.

22 T. Sanchez, D. T. N. Chen, S. J. DeCamp, M. Heymann and Z. Dogic, Nature, 2012, **491**, 431–434.

23 G. Henkin, S. J. DeCamp, D. T. N. Chen, T. Sanchez and Z. Dogic, Philosophical Transactions of the Royal Society A: Mathematical, Physical and Engineering Sciences, 2014, **372**, 20140142–20140142.

24 T. Sanchez, D. Welch, D. Nicastro and Z. Dogic, Science, 2011, **333**, 456–459.

25 F. Hilitski, Ph.D. thesis, Brandeis University, 2017.

26 T. Gao, R. Blackwell, M. A. Glaser, M. D. Betterton and M. J. Shelley, Physical Review E, 2015, **92**, year.

27 C. L. Kane and T. C. Lubensky, Nature Physics, 2013, **10**, 39–45.

28 A. W. Lees and S. F. Edwards, Journal of Physics C: Solid State Physics, 1972, **5**, 1921.

29 A. Nicolas, K. Martens, L. Bocquet and J.-L. Barrat, Soft Matter, 2014, **10**, 4648–4661.

30 G. Picard, A. Ajdari, F. Lequeux and L. Bocquet, Phys. Rev. E, 2005, **71**, 010501.

31 R. L. Stratonovich, SIAM Journal on Control, 1966, **4**, 362–371.
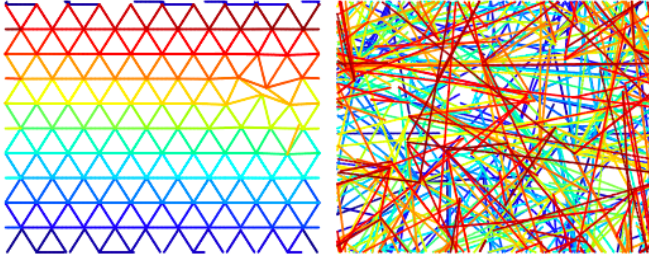
We study the impact of effects strongly non-affine effects and states of "self-stress" on transient active networks.